Available online at www.sciencedirect.com

ScienceDirect

www.elsevier.com/locate/jes

JES JOURNAL OF ENVIRONMENTAL SCIENCES

www.jesc.ac.cn

Polytitanium sulfate (PTS): Coagulation application and Ti species detection

Yanxia Zhao[1,3], *Sherub Phuntsho*[2], *Baoyu Gao*[1,*], *Hokyong Shon*[2,*]

1. *Shandong Key Laboratory of Water Pollution Control and Resource Reuse, School of Environmental Science and Engineering, Shandong University, Jinan 250100, China*
2. *Centre for Technology in Water and Wastewater, School of Civil and Environmental Engineering, University of Technology, Sydney, Broadway, NSW 2007, Australia*
3. *Key Laboratory for Special Functional Aggregated Materials of Education Ministry, School of Chemistry and Chemical Engineering, Shandong University, Jinan 250100, China*

ARTICLE INFO

Article history:
Received 29 February 2016
Revised 1 April 2016
Accepted 20 April 2016
Available online 5 May 2016

Keywords:
Polytitanium sulfate
Coagulation and flocculation
Titanium species
Floc properties

ABSTRACT

Interest in the development of inorganic polymerized coagulants is growing; however, there are only limited studies on the synthesis of polytitanium coagulants, which are expected to exhibit improved coagulation efficiency with better floc properties. This study presents the synthesis of polytitanium sulfate (PTS) for potential application in water purification, followed by characterization of PTS flocs and titanium species detection. Stable PTS solutions were successfully synthesized and standard jar tests were conducted to evaluate their coagulation efficiency. Electrospray ionization time-of-flight mass spectrometry (ESI-TOF-MS) speciation analysis revealed that a variety of mononuclear and polynuclear complexes were formed in PTS solution, indicating the polymeric nature of the synthesized coagulant. Floc characteristics were studied through on-line monitoring of floc size using a laser diffraction particle size analyzer. Results showed that PTS had a comparable or in some cases even higher organic matter and particulate removal efficiency than $Ti(SO_4)_2$. The effluent pH after PTS coagulation significantly improved toward desirable values closer to neutral pH. Properties of flocs formed by PTS were significantly improved in terms of floc size, growth rate and structure. This study showed that PTS could be an efficient and promising coagulant for water purification, with the additional benefit that its coagulated sludge can be used to recover valuable TiO_2 nanoparticles for various commercial applications.

Introduction

Coagulation–flocculation is commonly used in water treatment (Hu et al., 2006). Utilizing conventional aluminum (Al) and iron (Fe) salts as coagulants, however, has two major issues: toxicity from the residual coagulant and production of huge volumes of sludge that needs to be safely disposed (Cheng and Chi, 2002). To overcome the sludge disposal problem, novel Ti-based salts have been proposed as coagulants for water purification (Shon et al., 2007; Yousef, 2009; Zhao et al., 2011a). The most significant advantage of using Ti-based coagulants is that the final coagulated sludge could

* *Corresponding authors.* E-mails: baoyugao_sdu@aliyun.com (Baoyu Gao), Hokyong.Shon-1@uts.edu.au (Hokyong Shon).

http://dx.doi.org/10.1016/j.jes.2016.04.008
1001-0742 © 2016 The Research Center for Eco-Environmental Sciences, Chinese Academy of Sciences. Published by Elsevier B.V.

be recovered to produce valuable titanium dioxide (TiO_2) nanoparticles as a byproduct (Hoffmann et al., 1995), which are expected to be a high-demand material in the future.

The study of Ti-based coagulants for water treatment has been reported in earlier studies (Wu et al., 2011; Zhao et al., 2011a). They have been observed to perform better than or at least comparable to the conventional Al and Fe salts in terms of particle and natural organic matter (NOM) removal efficiencies. Furthermore, the decantability of the settled flocs formed by Ti-based coagulants is higher than that of conventional coagulants, due to the formation of much larger floc sizes as well as higher floc growth rate. This therefore shortens the sludge retention time, resulting in a more compact sedimentation tank in the coagulation–flocculation process. Moreover, titanium compounds are reported to have no adverse toxicity effects (Emsley, 2001), for which reason they are rarely included in water quality guidelines. Overall, titanium-based coagulants have significant potential benefits as alternative coagulants to regular Al and Fe coagulants.

Recently, the development of pre-hydrolyzed Al- and Fe-based inorganic coagulants such as polyaluminum chloride (PAC), polyferric chloride (PFC) and polyferric sulfate (PFS) has received wide attention (Cao et al., 2011; Cheng and Chi, 2002; Gao et al., 2005; Jiang and Graham, 1998; Moussas and Zouboulis, 2009; Zouboulis et al., 2008). On the one hand, the pre-hydrolysis of Al or Fe ions occurs during the preparation stage, reducing the need for pH adjustment. On the other hand, the pre-hydrolyzed coagulants are less sensitive to temperature and are highly effective for water treatment.

When Ti salts are used directly as coagulants, H^+ ions are released due to titanium hydrolysis (Shon et al., 2007), resulting in low effluent pH values (3.5 to 5.0), which then necessitates substantial pH adjustment. Following earlier studies on inorganic polymeric coagulants, such as PAC, PFC and PFS, it is speculated that the low and narrow pH range resulting from titanium coagulation may be solved by developing polytitanium salts, which could minimize the H^+ release through pre-hydrolyzation of Ti species. This encouraged us to develop and report the synthesis of polytitanium chloride (PTC) in our earlier study (Zhao et al., 2013). PTC was found to be superior to the $TiCl_4$ coagulant in terms of particle and NOM removal, and in addition the effluent pH was efficiently improved by use of PTC. Researchers have reported the application of $Ti(SO_4)_2$ coagulants in water treatment (Wu et al., 2011; Yousef, 2009), while the synthesis of polytitanium sulfate (PTS) has been rarely reported so far. Following our successful development of PTC, the aim of this study is to develop stable and efficient PTS as a coagulant. Coagulation–flocculation using PAC and PFS can serve as a prototype for modeling PTS coagulant behavior.

After coagulant addition, the metal species formed in water play an important role in the coagulation–flocculation process. Electrospray ionization mass spectrometry (ESI-MS) was used to determine the metal species and has proved suitable for the detection of Al species in $AlCl_3$ and PAC coagulant solutions (Sarpola, 2007; Truebenbach et al., 2000). In the same manner, the distribution and transformation pattern of Ti species in $Ti(SO_4)_2$ and PTS coagulant solutions can be expected to be identified by ESI-MS. An understanding of the distribution of hydrolyzed Ti species would be of great assistance in developing highly efficient coagulants and in understanding their coagulation mechanisms.

The main objectives of this study are therefore to: (1) synthesize PTS coagulants with different B values (OH/Ti molar ratio) and identify the species formed in pre-hydrolyzed Ti coagulant solutions using electrospray ionization time-of-flight mass spectrometry (ESI-TOF-MS), (2) evaluate the performance of PTS for both synthetic and real water treatment, (3) characterize the floc properties using a laser diffraction instrument and (4) identify the treatment mechanisms involved in the coagulation–flocculation process.

1. Experimental

1.1. PTS preparation

The PTS was synthesized using a slow alkaline titration method by adding a pre-determined amount of concentrated NaOH) solution (200.0 g/L) slowly into $Ti(SO_4)_2$ solution (≥24%, ρ = 1.33 g/mL, Kanto Chemical Co. Inc., Tokyo, Japan). The addition rate was 0.5 mL/min and the mixing speed was maintained at 700–800 r/min using a magnetic stirrer. The chosen B (OH/Ti molar ratio) values were 0.1, 0.3, 0.5, 1.0, 1.5, 2.0, 2.5, 3.0, 4.0 and 5.0; irreversible $Ti(OH)_4$ precipitation occurred at the final stage of titration for higher values of B. Resultant samples were denoted as PTS_{01}, PTS_{03}, PTS_{05}, PTS_{10}, PTS_{15}, PTS_{20}, PTS_{25}, PTS_{30}, PTS_{40} and PTS_{50}, respectively. Photos of the coagulants with aging period are presented in Appendix A Fig. S1.

Table 1 – Characteristics of water samples and measurement methods.

Characteristics	SW	RW	Measurement method
Turbidity (NTU)	4.75–5.33	1.30–3.19	Turbidimeter (Hanna, HI93414)
Ultraviolet light absorption at 254 nm (UV_{254}) (cm^{-1})	0.331–0.344	0.185–0.189	Prefiltered sample measured on a UV-1700 UV–VIS spectrophotometer (Shimadzu, Japan)
Dissolved organic carbon (DOC) (mg/L)	5.14–5.58	7.76–9.28	Prefiltered sample measured on a TOC analyzer (multi N/C 3100 analyzer, Analytical Jena)
Zeta potential (mV)	−18.0 to −19.0	−15.3 to −15.7	Nano ZS (ZEN 3600, Malvern, UK)
pH	8.06–9.07	7.46–8.03	pH analyzer (Hanna, HI991003)

SW: synthetic water containing humic acid (HA) as model NOM Australia.
RW: river water from Parramatta, Sydney.

1.2. Test water and jar-test

Coagulation experiments were performed using: (1) synthetic water (SW) containing humic acid (HA) as model NOM, and (2) river water (RW) from Parramatta, Sydney, Australia. Standard jar tests were conducted using a programmable jar-tester. Details of the experimental procedures are described in Appendix A S2 and characteristics of water samples are presented in Table 1.

1.3. Determination of dynamic floc properties

A laser diffraction instrument (Mastersizer 2000, Malvern, UK) was used for on-line measurement of dynamic floc size. The schematic diagram of the on-line monitoring system for measuring dynamic floc size can be referred to Zhao et al. (2011b). Floc growth rate was calculated from the slope of the rapid growth region as follows (Xiao et al., 2010):

$$\text{Growth rate} = \frac{\Delta \text{size}}{\Delta \text{time}} \quad (1)$$

Following the floc growth phase, the aggregated flocs were exposed to shear force at 200 r/min for 1 min, followed by a further 15 min of slow mixing at 40 r/min to allow floc regrowth. Floc strength factor (S_f) and recovery factor (R_f) are widely used to compare the relative floc breakage and recoverability, as calculated in the following equations (Cao et al., 2011; Jarvis et al., 2005):

$$S_f = \frac{d_2}{d_1} \times 100\% \quad (2)$$

$$R_f = \frac{d_3 - d_2}{d_1 - d_2} \times 100\% \quad (3)$$

where d_1 is the average floc size at the plateau region before breakage, d_2 is the floc size after the floc breakage period, and d_3 is the floc size after regrowth to a new plateau.

Flocs with larger S_f are stronger than those with lower S_f. Likewise, flocs with larger R_f show better recoverability after high shear.

Fractal geometry has been widely used to describe particle structure. The aggregate structures can be simply described by the fractal dimension D_f (Jarvis et al., 2005). Previous studies have reported the determination of the aggregate mass fractal dimension by a small-angle laser light scattering technique using the Mastersizer 2000 instrument (Jarvis et al., 2005; Lin et al., 2008). The total scattered light intensity I, the scattering vector Q, and D_f follow a power law as shown in the following equation (Rieker et al., 2000):

$$I \propto Q^{-D_f} \quad (4)$$

The scattering vector Q is the difference between the incident and the scattered wave vectors of the radiation beam in the medium expressed as (Lin et al., 2008):

$$Q = \frac{4n\pi \sin(\theta/2)}{\lambda} \quad (5)$$

where n, λ and θ are the refractive index of the medium, the laser light wavelength in vacuum, and the scattering angle, respectively.

As reported previously (Cao et al., 2011), flocs with open structure have low D_f values, whereas high D_f values generally indicate more compact structures.

1.4. Electrospray ionization time-of-flight mass spectrometry

The pre-hydrolyzed Ti species were analyzed using ESI-TOF-MS. Mass spectra were recorded with a high performance liquid chromatography/hybrid quadrupole time-of-flight mass spectrometer (Micromass Q-TOF Micro, Waters, USA). The detailed instrumental conditions can be referred to the study by Sarpola (2007).

2. Results and discussion

2.1. Performance of PTS coagulation for SW treatment

Newly-prepared PTS solutions were evaluated for their coagulation efficiency in SW treatment in terms of residual turbidity, UV_{254} absorbance, dissolved organic carbon (DOC), floc zeta potential and effluent pH (Fig. 1). Parallel experiments using $Ti(SO_4)_2$ (PTS_0) were conducted as reference.

Both UV_{254} and DOC removal efficiency showed insignificant variation with B value of up to 2.5, while beyond this B value, an obvious reduction in coagulation efficiency was observed. Residual turbidity decreased gradually with the increase in B value, reaching the lowest value of 2.17 nephelometric turbidity units (NTU) at the B value of 1.5. Beyond this B value, however, the residual turbidity showed an increasing trend. The distinct increase in residual turbidity and decrease in UV_{254} and DOC removal at B values higher than 2.5 demonstrated that the pre-hydrolyzed polymeric Ti species were less efficient for HA removal than the Ti species formed *in situ* by PTS_0. When the B value was increased from 0 to 1.5, the floc zeta potential decreased slightly, from +2.1 to −0.6 mV. However, when the B value was further increased, a significant decrease in floc zeta potential was seen. The increase of B value was accompanied by an increase in effluent pH, indicating that the development of PTS minimized H^+ release through the pre-hydrolysis of Ti species.

PTS_0 achieved high HA removal mainly by charge neutralization, through reaction between the *in situ* formed hydrolyzed Ti species and the negatively-charged HA molecules. However, the positively-charged Ti species were expected to be sufficient for charge neutralization, resulting in the floc zeta potential of +2.1 mV due to the redundant hydrolyzates attached to the particle surface. The PTS samples with B value from 0.1 to 1.5 achieved complete charge neutralization, producing flocs with zeta potential close to 0 mV. The apparent decrease of floc zeta potential at B > 1.5 indicated that the pre-hydrolyzed Ti species did not satisfy complete charge neutralization, demonstrating their relatively weak charge neutralization ability. The resultant flocs had negative zeta potentials, and thus sweep flocculation may be the dominant mechanism for HA removal. Bulk and rapid hydrolysis may occur at high B values (at B ≥ 3.0), producing Ti species with less positive charges, probably including $Ti(OH)_4$ and $Ti(OH)_5^-$. The high residual turbidity of up to 20.0 NTU may be attributed to repulsion among flocs with similar charges, while the decrease in UV_{254} and DOC removal efficiency could be ascribed to the weak charge neutralization capability.

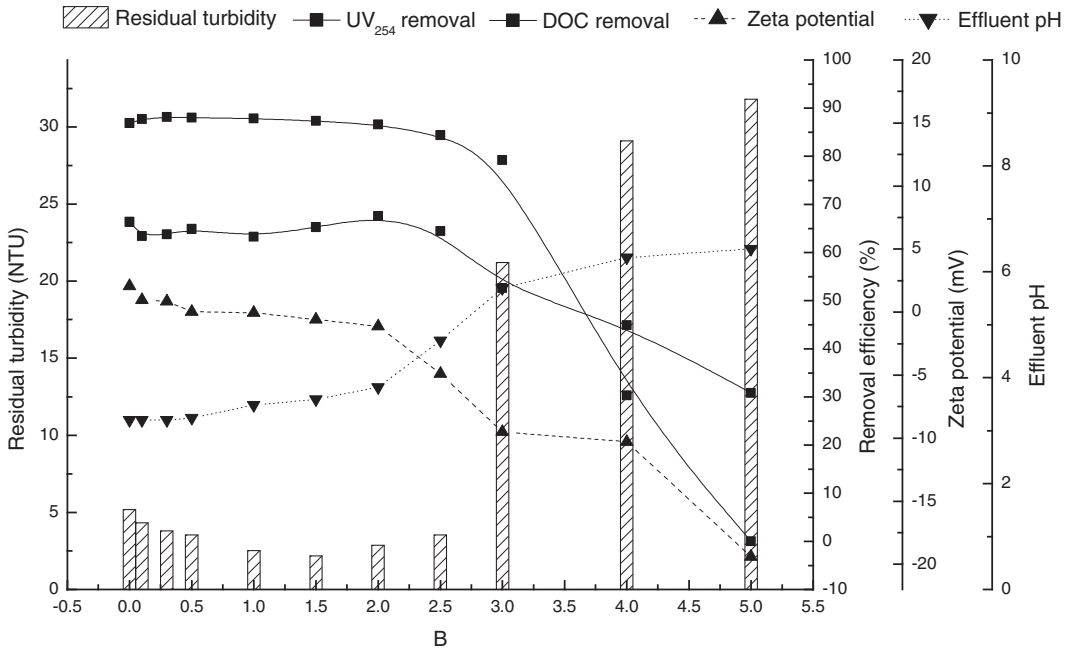

Fig. 1 – Coagulation performance of polytitanium sulfate in terms of residual turbidity, UV_{254} removal, dissolved organic carbon removal, floc zeta potential and effluent pH under various B value conditions (coagulant dose 10 mg-Ti/L).

Previous studies on PAC have reported that the polymeric Al species are metastable, and Al_{13} is known to be the most effective and stable polymeric compound for water purification (Smith, 1971). Accordingly, the initially-formed hydrolyzates of PTS may only be transitional species, which would slowly convert to more stable species during aging. However, the intensive hydrolysis at high B values deteriorated the stability of PTS solutions and resulted in precipitates, as shown in Appendix A Fig. S1.

2.2. Coagulation kinetics and floc properties for SW treatment

2.2.1. Floc size and growth rate

As shown in Fig. 2a, no appreciable flocs were formed with PTS_{40} and PTS_{50} coagulants during the floc growth phase, and this was evident from the corresponding high residual turbidity and low HA removal efficiency, as shown in Fig. 1. In all other cases, the floc size significantly increased after slow mixing at 40 r/min. There was a significant drop in floc size after the introduction of high shear force (200 r/min), followed by a gradual floc regrowth when the shear force was restored to 40 r/min. However, the flocs could not regrow to their previous size.

Fig. 2b shows the variation of both floc growth rate and floc size with B value. Results suggested that the floc sizes d_1, d_2 and d_3 increased with increasing B value, reaching a plateau at high B values for d_1 and d_3. The variation of floc growth rate with B value showed a parabolic trend with the inflection point at B = 2.0, at which point PTS achieved the highest floc growth rate of 193.5 μm/min. The increase of floc size and floc growth rate at higher B values demonstrated that the pre-hydrolyzed Ti polymer may have a chain structure, which favored charge neutralization and complexation by bridging and/or adsorption of HA molecules onto the pre-hydrolyzates. The higher floc growth rate by PTS at higher B values was consistent with the assumption that the preformed species can destabilize particles more quickly (Matsui et al., 1998).

2.2.2. Floc strength factor (S_f), recovery factor (R_f) and fractal dimension (D_f)

As shown in Fig. 2a, once shear was applied, the floc size decreased dramatically, followed by floc re-aggregation as the shear was reduced again. The S_f and R_f were calculated according to Eqs. (2) and (3), and the results are plotted in Fig. 2c. The variation of S_f with B value was inconsistent, while R_f gradually decreased with increasing B value but showed an increasing trend at B > 2.5. As previously noted, the dominant coagulation mechanism changed from charge neutralization to sweep flocculation at high B values, which corresponded well with the decrease in R_f at B < 2.5. The flocs formed by sweep flocculation were reported to show poor floc regrowth after breakage (Aguilar et al., 2003). However, a sharp increase in R_f was seen at B > 2.5. The PTS samples with high B values were likely to include a high content of pre-hydrolyzed polymer, which could bond the floc fragments due to their bridging ability and result in R_f increase. The flocs produced by bridging flocculation were larger than those formed simply by charge neutralization, and hence promoted by further aggregation (Ray and Hogg, 1987). This provided a further explanation for the increase in floc size at high B values. The flocs formed at all B values showed irreversible breakage, as reflected by both S_f and R_f values being below 100%. This indicated that charge neutralization was not the sole mechanism, but that sweep flocculation also played a significant role in the coagulation process. Flocs formed by charge neutralization should exhibit total recovery, while those

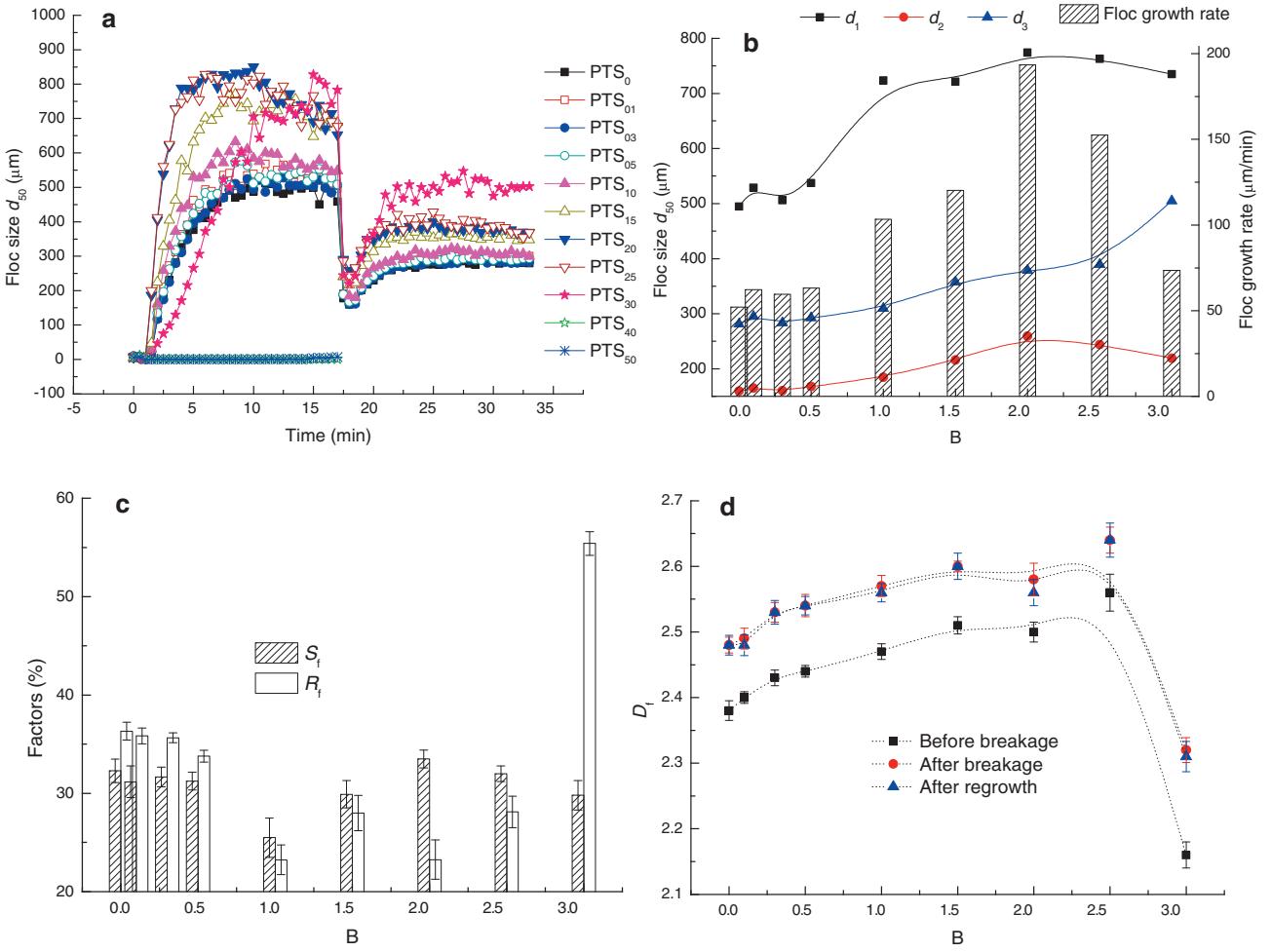

Fig. 2 – Flocs formed by polytitanium sulfate with different B values: (a) floc growth, breakage and regrowth profiles, (b) floc size (d_1, d_2 and d_3) and floc growth rate, (c) floc S_f, R_f and (d) D_f under different B value conditions.

formed by sweep flocculation are likely to exhibit reduced recovery from shear-induced breakup (McCurdy et al., 2004). The recoverability of flocs also provides an indication of the internal bonding structure of the floc (Jarvis et al., 2005). The irreversible floc breakage with limited floc growth (Fig. 2a) was seen as evidence that the flocs formed were held together by chemical bonding rather than physical bonding.

As shown in Fig. 2d, the variation of D_f with B value showed a parabolic trend with the inflection point at the B value of 2.5, at which point the resultant flocs had the largest D_f value and therefore the most compact structure. For PTS_0, instant hydrolysis occurred after $Ti(SO_4)_2$ addition into water, followed by the reaction between *in situ* formed Ti hydrolyzates and HA molecules, producing insoluble primary flocs. For PTS with high B values, the pre-hydrolyzed Ti species were expected to react directly with HA, resulting in the formation of different primary flocs compared to those formed by Ti species formed *in situ*. For PTS with $B < 2.5$, the gradual increase in D_f with increasing B value indicated that the primary flocs may be more attached to one another, or that the interior repulsion between flocs was reduced, and therefore flocs with high compactness were produced. However, a sharp decrease in D_f was seen for B values larger than the inflection point (2.5), indicating the possibility that the pre-hydrolyzed polymers at high B values may favor an extended conformation away from the interface, thus yielding flocs with an open structure (Hopkins and Ducoste, 2003). Flocs became more compact upon exposure to high shear as they broke at their weakest points and possibly rearranged into more stable structures (Tang et al., 2002). The PTS flocs showed this expected change in compaction as indicated by the substantial increase in floc D_f when flocs were broken into smaller units and subsequently formed a more compact structure.

2.3. *Coagulation performance optimization for SW treatment*

PTS_{15} achieved UV_{254} and DOC removal comparable to those of PTS_0, but showed superiority with respect to turbidity removal (Fig. 1). Also, the resultant flocs exhibited larger sizes with higher floc growth rate, and a more compact structure. Thus, PTS_{15} was selected as the optimum PTS coagulant for HA removal and was utilized in further research. The coagulation optimization performance of PTS_{15} and PTS_0 was investigated for comparison to ascertain the optimum coagulant dose and initial solution pH for HA removal, with detailed information provided in S3.

For both PTS_{15} and PTS_0, the optimum coagulant dose was selected as 10 mg/L, and the optimum solution pH was chosen as pH 9. The coagulation efficiency of PTS_{15} and PTS_0 and the selected floc characteristics are summarized in Table 2. Results showed that the PTS_{15} coagulant was more favorable for turbidity removal, while the organic matter removal was comparable to that by PTS_0. The PTS_{15} produced flocs with larger d_1, d_2 and d_3 than those produced by PTS_0. The floc growth rate for the PTS_{15} coagulant was 125.7 μm/min, double that for PTS_0, which agreed with the assumption that the preformed species destabilize particles more rapidly (Matsui et al., 1998). The flocs formed by PTS_{15} and PTS_0 presented comparable abilities to resist shear, as reflected by comparable S_f values, however the flocs for PTS_{15} had weaker re-formation capability as evidenced by their lower R_f value. Floc zeta potentials were close to zero under optimum conditions, which confirmed complete charge neutralization. The R_f values of the flocs produced by PTS_{15} and PTS_0 were both below 100%, indicating that sweep flocculation also played an active role during the coagulation process apart from charge neutralization. Since the same artificial water was used in this study as that in our previous publication (Zhao et al., 2015), a comparison between PTS_{15} and regular PAC was carried out (see Appendix A S5). The novel PTS with optimum B value of 1.5 was superior to conventional PAC and gave higher organic matter removal and improved floc properties in terms of floc growth rate and floc size (regardless of d_1, d_2 and d_3); whereas the flocs formed by PTS had weak recoverability and comparable floc strength to those formed by PAC, which is in agreement with previous conclusions from a comparison between Ti-based coagulants and Al-based coagulants (Zhao et al., 2011b).

Fig. 3 shows the evolution of floc size and the change in D_f over time during floc growth, breakage and regrowth processes. For both PTS_{15} and PTS_0, D_f increased gradually with time during the floc growth period, reaching 2.56 and 2.39, respectively. A significant increase in D_f was observed when a high shear rate of 200 r/min was applied, and the value increased to 2.64 and 2.49 for PTS_{15} and PTS_0, respectively, at the end of the breakage process. This can presumably be ascribed to the fact that the weak points of aggregates were ruptured by high shear speed, and were then rearranged at more favorable points (Hopkins and Ducoste, 2003; Selomulya et al., 2001). Additionally, little variation in D_f was observed during the floc regrowth period, and the value was comparable to that at the end of the breakage period. Larger floc size generally results in smaller fractal dimension (Cao et al., 2011); however the PTS_{15} yielded flocs with a more compact structure than PTS_0 given the higher D_f values, regardless of floc growth, breakage or regrowth processes, although the flocs formed by PTS_{15} were larger than those formed by PTS_0. The flocs formed by the pre-hydrolyzed Ti species therefore exhibited a higher degree of compaction than those formed by

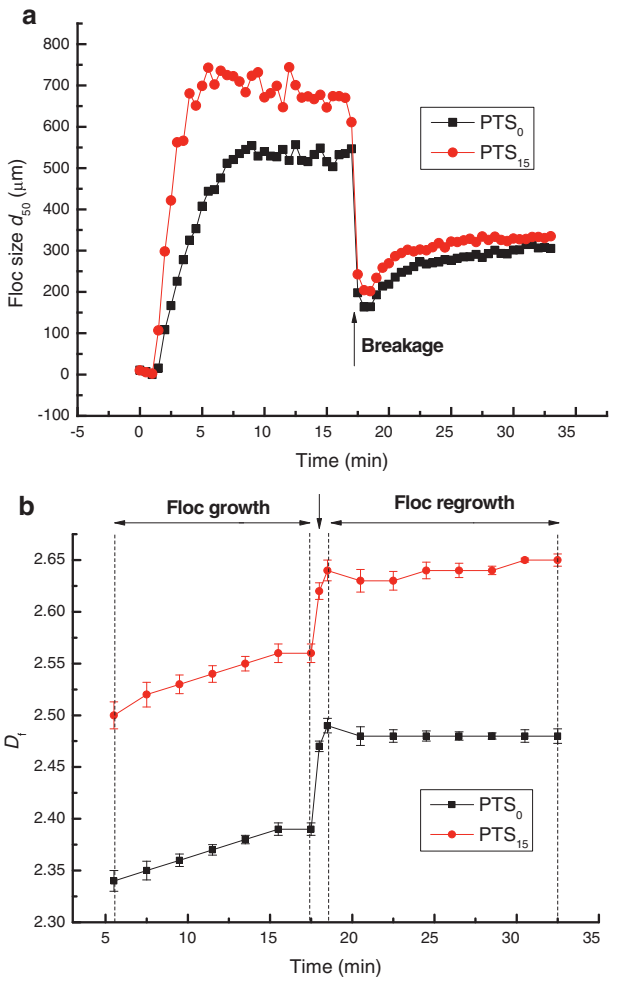

Fig. 3 – Change of floc size (a) and floc D_f (b) vs. coagulation time during floc growth, breakage (200 rpm for 1 min) and regrowth processes under the optimum coagulant dose and solution pH conditions (the optimum coagulant dose was 10 mg-Ti/L, while the optimum solution pH before coagulation was pH 9).

Ti species formed *in situ*, which was of great significance for water purification since D_f is an important parameter influencing floc density and affecting solid/liquid separation (Gregory, 1998).

2.4. Performance of PTS coagulation in RW treatment

The coagulation performance of PTS was tested in RW treatment and the results are presented in Appendix A S6. Results suggested that PTS increased the residual turbidity,

Table 2 – Comparison of floc properties between PTS_0 and PTS_{15} under optimum coagulant dose and solution pH conditions (the optimum coagulant dose: 10 mg/L, optimum solution pH: 9).

Coagulant	Residual turbidity (NTU)	UV_{254} removal (%)	DOC removal (%)	Zeta potential (mV)	Floc growth rate (μm/min)	d_1 (μm)	d_2 (μm)	d_3 (μm)	S_f (%)	R_f (%)
PTS_0	4.1	87.3	59.0	+0.9	62.7	532.6	163.7	298.3	30.7	36.5
PTS_{15}	2.4	87.7	62.3	+0.1	125.7	691.2	202.1	328.3	29.2	25.8

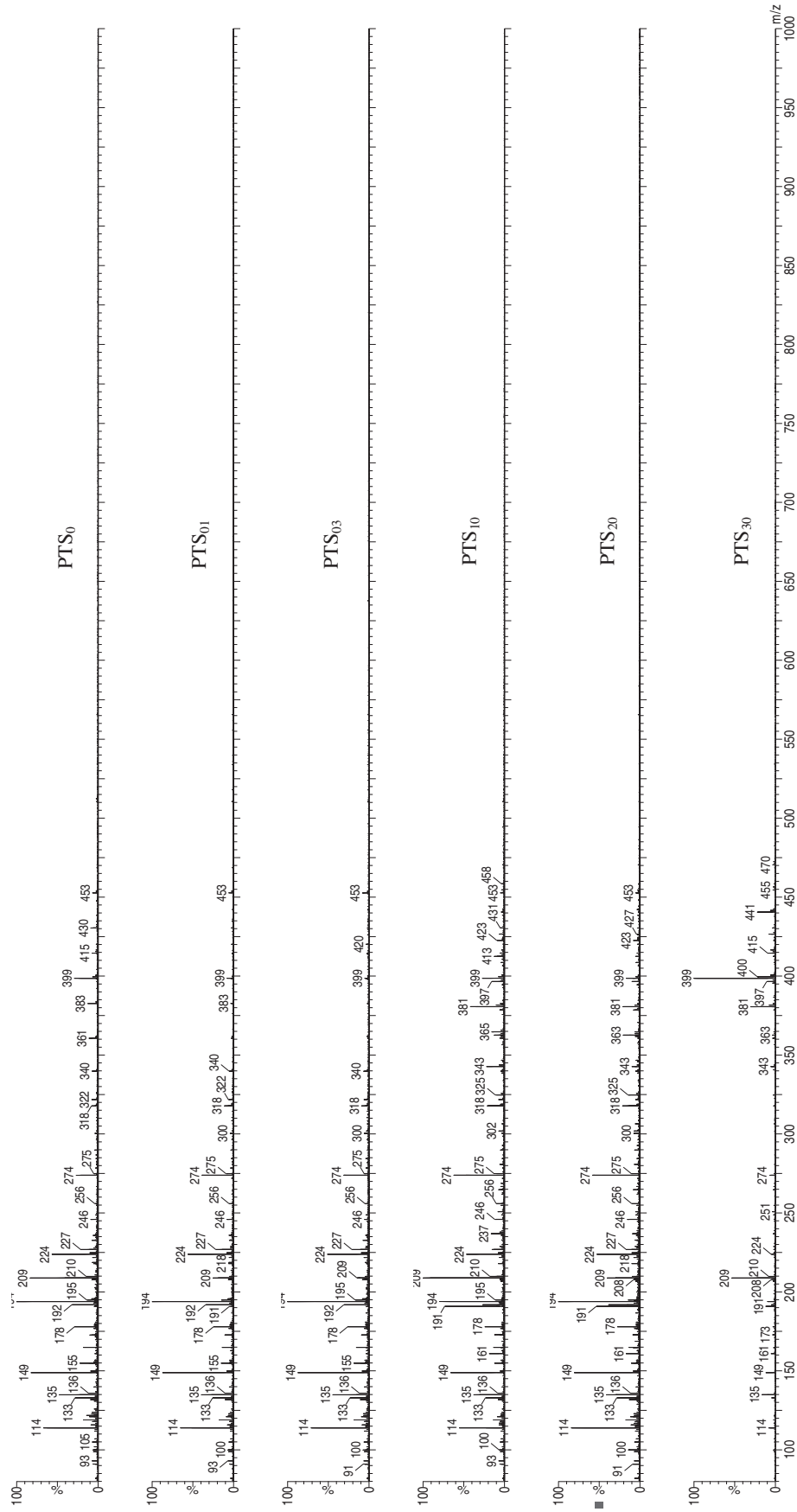

Fig. 4 – Electrospray ionization time-of-flight mass spectrometry of hydroxyl Ti solutions with different B values (PTS_0, PTS_{01}, PTS_{03}, PTS_{10}, PTS_{20}, PTS_{30}).

especially at high coagulant doses. Significant improvement in UV_{254} and DOC removal was observed at higher B values. Compared to $Ti(SO_4)_2$, PTS_{30} improved the UV_{254} and DOC removal by up to 7.0% and 10.0%, respectively. Additionally, the effluent pH increased with increasing B value, which was in agreement with the results obtained in Section 2.1. Kinetic growth, breakage and regrowth of flocs formed by PTS under different B value conditions are presented in Appendix A Fig. S9. Little variation in floc size d_1 (around 960–980 μm) was observed for PTS at different B values. Compared to $Ti(SO_4)_2$, the floc sizes d_2 and d_3 were improved to different degrees for PTS, resulting in the variation of floc strength and recoverability. PTS_{03} produced flocs with S_f of about 75.5%, which was 43.4% higher than flocs produced by $Ti(SO_4)_2$, while the floc R_f was enhanced from 12.3% to 46.0%.

2.5. Ti species detection experiments

The ESI-TOF-MS spectra of PTS solutions at different B values are presented in Fig. 4. The Ti species were assigned according to their mass to charge ratio (*m*/z). The Ti complex was mainly composed of Ti^{4+}, O^{2-}, OH^-, HSO_4^-, SO_4^{2-} and H_2O, and therefore $[Ti_aO_b(OH)_c(HSO_4)_x(SO_4)_y(H_2O)_z]^{(4a-2b-c-x-2y)+}$ was suggested as the general formula for all the species in the present study. The proposed cationic Ti complexes at different *m*/z values can be found in Appendix A Table S2 and written as structural formulas. However, not all possible species are listed in this table. There are ambiguities in the assignments of signals to a given formula, since the same *m*/z values can correspond to different species. For instance, in the following cases: $(OH)_2^{2-}$ and $O(H_2O)^{2-}$, $((SO_4)(OH))^{3-}$ and $(O(HSO_4))^{3-}$, $((SO_4)(H_2O))^{2-}$ and $((OH)(HSO_4))^{2-}$, $(OH)_4^{4-}$ and $(O_2(H_2O))^{4-}$ have identical *m*/z values but different structural formulas.

When the B value increased from 0 to 2.0, no significant difference in the mass spectra was observed for the main signals. The distribution of main signals at different B values is presented in Table 3. For PTS_0, PTS_{01}, PTS_{03} and PTS_{20}, the species at *m*/z of 194 dominated the mass spectra with an intensity of 100%, while for PTS_{10}, the most intense peak appeared at *m*/z of 209. When B was increased to 1.0 and 2.0, the peak intensity at *m*/z = 274 and 318 increased by around 50% compared to PTS_0, PTS_{01} and PTS_{03}, and peaks at *m*/z = 343 and 381 began to appear. As shown in Appendix A Table S2, the Ti species at *m*/z of 343 and 381 contained more titanium atoms, *e.g.*, Ti_7, Ti_8, Ti_9 and Ti_{10}. It can therefore be concluded that, with increasing B value, the hydrolysis of the $Ti(SO_4)_2$ coagulant promoted the process of polymerization. The mass spectrum of PTS_{30} was significantly different from that of PTS at B < 3.0. The Ti species at *m*/z of 399 dominated the mass spectra, whereas the signal intensity at *m*/z of 114, 135, and 274 apparently decreased, and the signals at *m*/z of 178 and 194 vanished. At B = 3.0, Ti species may further hydrolyze to large polymers, reflected by the new signal observed at *m*/z = 441 with intensity of 22% (Table 3). This corresponded well with flocs formed by PTS_{30} having the highest R_f values, as shown in Fig. 2c. As previously mentioned, a high content of pre-hydrolyzed polymers was expected to bond the floc fragments via bridging after floc breakage and therefore resulted in high R_f.

Table 3 – Distribution of main signals (relative ion strength) in the ESI-TOF-MS at different B value conditions.

m/z	Intensity (%)					
	PTS_0	PTS_{01}	PTS_{03}	PTS_{10}	PTS_{20}	PTS_{30}
114	68	68	71	55	84	8
135	47	40	44	38	41	17
149	81	88	87	66	80	12
178	33	26	34	24	28	–
194	100	100	100	83	100	–
209	81	25	14	100	40	54
224	57	56	51	47	53	–
274	26	38	31	62	58	7
318	8	11	9	21	21	–
343	–	–	–	22	10	6
381	–	–	–	42	21	31
399	28	–	–	27	17	100
441	–	–	–	–	–	22

The Al species in PAC solutions have been previously identified using ESI-TOF-MS (Feng et al., 2011). One major difference in the mass spectra of PTS to the chloride system is the lack of a Gaussian distribution of signals (with a difference of 18 u), which indicates how many aquo ligands are attached to one species and help to confirm the charges of the species (Sarpola, 2007). This observation indicates the different pathway of Ti polymerization to form polymeric species in the presence of sulfate ions. As revealed in Appendix A Table S2, almost all the main species of PTS identified in this study contained sulfate or hydrogen sulfate. It can be concluded that the coagulation principle of PTS was different from that of PAC due to the remarkable role of sulfate anion, thus resulting in the differences between PTS and PAC in both coagulation efficiency and floc characteristics. The characteristics of Ti species in PTS solution still require investigation.

3. Conclusions

In this study, polytitanium sulfate (PTS) was synthesized as new coagulant through pre-hydrolysis of $Ti(SO_4)_2$. The performance of PTS in water purification was tested through standard jar tests. The hydrolyzed Ti species in PTS coagulant solutions were also identified using ESI-TOF-MS. The following conclusions are drawn from this particular study: (1) $Ti(SO_4)_2$ coagulant can be pre-hydrolyzed to form clear and stable PTS coagulants under certain ranges of basicity conditions. The PTS coagulant was found to be an efficient coagulant for water purification in terms of both particulate and organic matter removal. In addition, the treated water pH was significantly improved toward neutral pH, indicating that utilization of PTS could reduce H^+ release through pre-hydrolysis of Ti species and thereby reduce the need for pH adjustment in post treatment. (2) The PTS coagulants produced larger flocs with higher floc growth rate than non-pre-hydrolyzed $Ti(SO_4)_2$, suggesting that the PTS coagulant would require shorter retention time and more compact mixing and sedimentation tanks. The flocs formed by PTS also exhibited a higher degree of compaction, which was significant for final solid/liquid separation. (3) ESI-TOF-MS analysis evidenced the presence of various hydrolyzed Ti

species in PTS solution, indicating the successful polymerization during hydrolysis of $Ti(SO_4)_2$ coagulants under different B values.

Acknowledgments

This work was supported by the National Natural Science Foundation of China (Nos. 51278283 and 51508308), the China Postdoctoral Science Foundation (Nos. 2014M560557 and 2015T80722), and the Tai Shan Scholar Foundation (No. ts201511003) and Hong Kong Scholars Program.

Appendix A. Supplementary data

Supplementary data to this article can be found online at http://dx.doi.org/10.1016/j.jes.2016.04.008.

REFERENCES

Aguilar, M., Saez, J., Llorens, M., Soler, A., Ortuno, J., 2003. Microscopic observation of particle reduction in slaughterhouse wastewater by coagulation–flocculation using ferric sulphate as coagulant and different coagulant aids. Water Res. 37 (9), 2233–2241.

Cao, B., Gao, B., Liu, X., Wang, M., Yang, Z., Yue, Q., 2011. The impact of pH on floc structure characteristic of polyferric chloride in a low DOC and high alkalinity surface water treatment. Water Res. 45 (18), 6181–6188.

Cheng, W.P., Chi, F.H., 2002. A study of coagulation mechanisms of polyferric sulfate reacting with humic acid using a fluorescence-quenching method. Water Res. 36 (18), 4583–4591.

Emsley, J., 2001. Titanium. Nature's Building Blocks: An AZ Guide to the Elements. Oxford University Press, Oxford, England, UK, pp. 451–452.

Feng, C., Bi, Z., Zhao, S., Li, N., Wang, D., Tang, H., 2011. Quantification analysis of polymeric Al species in solutions with electrospray ionization time-of-flight mass spectrometry (ESI-TOF-MS). Int. J. Mass Spectrom. 309, 22–29.

Gao, B.Y., Chu, Y.B., Yue, Q.Y., Wang, B.J., Wang, S.G., 2005. Characterization and coagulation of a polyaluminum chloride (PAC) coagulant with high Al_{13} content. J. Environ. Manag. 76 (2), 143–147.

Gregory, J., 1998. The role of floc density in solid–liquid separation. Filtr. Sep. 35 (4) (367-366).

Hoffmann, M.R., Martin, S.T., Choi, W., Bahnemann, D.W., 1995. Environmental applications of semiconductor photocatalysis. Chem. Rev. 95 (1), 69–96.

Hopkins, D.C., Ducoste, J.J., 2003. Characterizing flocculation under heterogeneous turbulence. J. Colloid Interface Sci. 264 (1), 184–194.

Hu, C., Liu, H., Qu, J., Wang, D., Ru, J., 2006. Coagulation behavior of aluminum salts in eutrophic water: significance of Al_{13} species and pH control. Environ. Sci. Technol. 40 (1), 325–331.

Jarvis, P., Jefferson, B., Parsons, S.A., 2005. Breakage, regrowth, and fractal nature of natural organic matter flocs. Environ. Sci. Technol. 39 (7), 2307–2314.

Jiang, J., Graham, N., 1998. Observations of the comparative hydrolysis/precipitation behaviour of polyferric sulphate and ferric sulphate. Water Res. 32 (3), 930–935.

Lin, J.L., Huang, C., Chin, C.J.M., Pan, J.R., 2008. Coagulation dynamics of fractal flocs induced by enmeshment and electrostatic patch mechanisms. Water Res. 42 (17), 4457–4466.

Matsui, Y., Yuasa, A., Furuya, Y., Kamei, T., 1998. Dynamic analysis of coagulation with alum and PACl. J. Am. Water Works Assoc. 90 (10), 96–106.

McCurdy, K., Carlson, K., Gregory, D., 2004. Floc morphology and cyclic shearing recovery: comparison of alum and polyaluminum chloride coagulants. Water Res. 38 (2), 486–494.

Moussas, P., Zouboulis, A., 2009. A new inorganic–organic composite coagulant, consisting of polyferric sulphate (PFS) and polyacrylamide (PAA). Water Res. 43 (14), 3511–3524.

Ray, D., Hogg, R., 1987. Agglomerate breakage in polymer-flocculated suspensions. J. Colloid Interface Sci. 116 (1), 256–268.

Rieker, T.P., Hindermann-Bischoff, M., Ehrburger-Dolle, F., 2000. Small-angle X-ray scattering study of the morphology of carbon black mass fractal aggregates in polymeric composites. Langmuir 16 (13), 5588–5592.

Sarpola, A., 2007. The Hydrolysis of Aluminium, A Mass Spectrometric Study. University of Oulu, Oulu, Finland.

Selomulya, C., Amal, R., Bushell, G., Waite, T.D., 2001. Evidence of shear rate dependence on restructuring and breakup of latex aggregates. J. Colloid Interface Sci. 236 (1), 67–77.

Shon, H., Vigneswaran, S., Kim, I.S., Cho, J., Kim, G., Kim, J., et al., 2007. Preparation of titanium dioxide (TiO_2) from sludge produced by titanium tetrachloride ($TiCl_4$) flocculation of wastewater. Environ. Sci. Technol. 41 (4), 1372–1377.

Smith, R.W., 1971. Relations among equilibrium and nonequilibrium aqueous species of aluminum hydroxy complexes. Adv. Chem. Ser. 106 (2), 250–256.

Tang, P., Greenwood, J., Raper, J.A., 2002. A model to describe the settling behavior of fractal aggregates. J. Colloid Interface Sci. 247 (1), 210–219.

Truebenbach, C.S., Houalla, M., Hercules, D.M., 2000. Characterization of isopoly metal oxyanions using electrospray time-of-flight mass spectrometry. J. Mass Spectrom. 35 (9), 1121–1127.

Wu, Y.F., Liu, W., Gao, N.Y., Tao, T., 2011. A study of titanium sulfate flocculation for water treatment. Water Res. 45 (12), 3704–3711.

Xiao, F., Yi, P., Pan, X.-R., Zhang, B.-J., Lee, C., 2010. Comparative study of the effects of experimental variables on growth rates of aluminum and iron hydroxide flocs during coagulation and their structural characteristics. Desalination 250 (3), 902–907.

Yousef, O., 2009. Characterisation of titanium tetrachloride and titanium sulfate flocculation in wastewater treatment. Water Sci. Technol. 59 (12), 2463–2473.

Zhao, Y., Gao, B., Cao, B., Yang, Z., Yue, Q., Shon, H., et al., 2011a. Comparison of coagulation behavior and floc characteristics of titanium tetrachloride ($TiCl_4$) and polyaluminum chloride (PACl) with surface water treatment. Chem. Eng. J. 166 (2), 544–550.

Zhao, Y., Gao, B., Shon, H., Cao, B., Kim, J.H., 2011b. Coagulation characteristics of titanium (Ti) salt coagulant compared with aluminum (Al) and iron (Fe) salts. J. Hazard. Mater. 185 (2), 1536–1542.

Zhao, Y., Phuntsho, S., Gao, B., Huang, X., Qi, Q., Yue, Q., et al., 2013. Preparation and characterization of novel polytitanium tetrachloride coagulant for water purification. Environ. Sci. Technol. 47 (22), 12966–12975.

Zhao, Y., Phuntsho, S., Gao, B., Yang, Y., Kim, J.-H., Shon, H., 2015. Comparison of a novel polytitanium chloride coagulant with polyaluminium chloride: coagulation performance and floc characteristics. J. Environ. Manag. 147, 194–202.

Zouboulis, A., Moussas, P., Vasilakou, F., 2008. Polyferric sulphate: preparation, characterisation and application in coagulation experiments. J. Hazard. Mater. 155 (3), 459–468.